ELSEVIER

Chemical Engineering Journal 67 (1997) 205–214

Chemical Engineering Journal

Hydrodynamics and mass transfer studies in a novel external-loop airlift reactor

Y.X. Guo, M.N. Rathor, H.C. Ti *

Department of Chemical Engineering, National University of Singapore, 10 Kent Ridge Crescent, Singapore 119260

Received 18 November 1996; revised 26 March 1997; accepted 12 April 1997

Abstract

A novel external-loop airlift reactor in combination with a fluidized bed was proposed in this work. The gas sparger located in the upper section of the riser allowed the heavy solid particles to fluidize in the lower section of the riser, and also separated the gas–liquid and solid–liquid contact. The reactor, with high degree of design flexibility, is expected to handle fragile cells which are shear-sensitive. Studies were carried out using three different types of solid particles with three different solid loading in the reactor. The solids-free standard external-loop airlift reactors with different *H/D* ratio were also investigated for comparison. The gas holdup, liquid circulation velocity, liquid mixing time, and the fluidized-bed expansion were studied. Several models reported were applied to the hydrodynamic performance of the reactor. The oxygen transfer in the liquid was also measured and the k_La_L value was obtained using a dynamic technique. Empirical correlations describing the proposed reactor are presented in this paper and very good agreement could be found. © 1997 Elsevier Science S.A.

Keywords: External-loop airlift reactor; Fluidized bed; Gas holdup; Liquid circulation velocity; Mixing time; Volumetric oxygen transfer coefficient; Hydrodynamic; Mass transfer

1. Introduction

Nowadays, with the advantages of simple mechanical design, better mixing and improved power consumption, the airlift reactor has gained much attention from researchers and manufacturers. Numerous investigations have been made on the performance and characteristics of these reactors [1,2]. Nishikawa [3] and Allen and Robinson [4] studied the shear rate in airlifts, Chisti and Moo-Young [5,6] investigated the hydrodynamics and oxygen transfer in the reactor, and predicted liquid circulation velocity in airlift reactors with biological media. Bello et al. [7] focused on the liquid circulation and mixing characteristics of airlift contactors. Merchuk and Berzin [8] established a mathematical model based on the distribution of energy dissipation in the airlift reactors. For the airlift reactors containing three-phase flow (TPAL), the hydrodynamic behavior in internal-loops and multiphase mass transport in external-loops have been studied by Livingston and Zhang [9] and Mao et al. [10], respectively. Many workers [11–14] have paid much attention in the field of TPAL reactor investigations.

It has been shown that the external-loop airlift column has a high efficiency of homogenization and intense mixing, such that it can be used in biochemical application which involves highly viscous fluid [15]. However, it was reported by Murhammer and Goochee [16] that not only sparging can damage mammalian cells and insect cells, agitation may also have detrimental effects in animal cell bioreactors. In addition, the damage to cells on microcarriers is found to result from the power dissipation in the form of turbulent eddies. Their results suggested that cell damage can occur in the vicinity of the gas distributor and that bubble size and gas flow rate are not the only important considerations for cell damage in sparged bioreactors.

Apart from the airlift reactors, three-phase fluidized beds have also been suggested for applications in biochemical engineering [17]. The immobilization of living cells on fluidized carrier particles is an attractive method of achieving high cell viability and product yield. There are three main areas of application of biofluidization: (1) enzymes immobilized on a solid matrix; (2) biofluidization of pure cultures of whole cells immobilized on a solid matrix; (3) application of biofluidization to a wide variety of waste water treatment processes [18]. However, the power requirement is still high and many high shear intensity regions exist in the three-phase fluidized beds.

* Corresponding author. Tel: +874-2188; fax: +779-1936; e-mail: chetihc@leonis.nus.sg

PII S1385-8947(97)00043-0

It was therefore desirable to combine the advantages of a fluidized bed and airlift reactor to construct a novel reactor, which has the benefits of mechanical simplicity, good mixing, and lower liquid shear rates of the airlifts as well as the excellent liquid–solid contact, good heat and mass transfer of the fluidized beds. This novel reactor will be more suitable in biochemical processes.

The proposed reactor in this work is the combination of an external-loop airlift with a fluidized bed. The gas sparger is located in the middle of the riser, such that heavy particles are fluidized in the lower section of the riser. This design eliminates the high shear stress spots where direct contact of gas bubbles with the microcarrier will break the attachment of the cell from the carrier. Nikolov et al. [19], Garnier et al. [20] and Lele and Joshi [21] have reported the use of an inverse fluidized bed, by fluidizing light particles present in the downcomer of the airlift reactor. However, it is more popular to use heavy particles as the carrier in the biomass production, and in addition, a generalized model was not reported by them and thus their results can not be used. In the present work the hydrodynamic studies were carried out first to establish the feasibility and to characterize the behaviour of the proposed system. The correlation were obtained to describe the hydrodynamic properties of the reactor. Furthermore, the mass transfer rate for oxygen, a vital parameter for bioreactor design, was also investigated. The important volumetric mass transfer coefficient was calculated and compared with that of some other reactors. Three different types of solid particles were used in this study. The effects of solid loading, particle density, and the aerated height on the performance of the proposed reactor were investigated. The standard solid-free airlift reactor under otherwise identical conditions was also studied and the results compared with the three-phase system. The gas and liquid used in the reactor were air and water respectively.

2. Experimental setup

Fig. 1 shows the schematic diagram of the airlift fluidized-bed reactor, which was made of perspex materials. The dimensions of the reactor are listed in Table 1. The reactor had a degassed liquid volume of approximately 16.5×10^{-3} m^3, and a liquid height of 1.81 m, which was kept constant during the whole experiment. The sparger was 0.87 m under the unaerated liquid top level. The fluidized-bed column was located underneath the sparger, with the total working volume of 1.385×10^{-3} m^3.

Tap water and air were used as the sources for the liquid and gas phases in the experiment. The gas flowrate was measured using two rotameters with different ranges. The manometer was used to determine the gas holdup. The tracer response technique was applied to obtain the liquid circulation velocity and the mixing time in the reactor. Saturated NaCl solution was used as the tracer. The injection point was set at the top of the downcomer and the conductivity probes were introduced at various location along the downcomer. The output signal was recorded by a chart recorder. The mixing time was measured as the time required to achieve 100% homogeneity throughout the reactor. In order to distribute the tracer in the liquid uniformly, a thin tube was utilized as the syringe needle. The needle had a diameter of 2.7×10^{-3} m, and an effective length of 52×10^{-3} m, of which the tip-end was blocked. Six tiny holes, with 1.0×10^{-3} m diameter of the largest at the tip and 0.5×10^{-3} m of the smallest at the rear, were drilled on the tube.

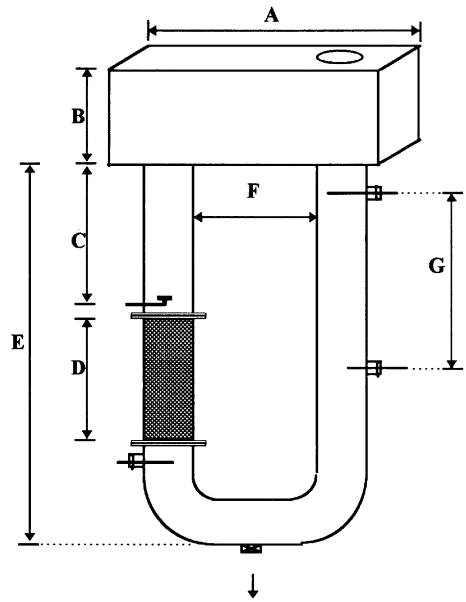

Fig. 1. Schematic diagram of the airlift fluidized-bed reactor.

Table 1
Dimensions of the airlift fluidized-bed reactor

Label	*m*	Label	*m*
A	0.497	F	0.327
B	0.200	G	0.793
C	0.867	Sparger diameter	0.022
D	0.490	Internal diameter	0.060
E	1.753	A_r/A_d	1

The volumetric mass transfer coefficient k_La_L was determined by a dynamic technique. The water in the reactor was first purged with nitrogen until the oxygen content became negligible, then the air was switched into the reactor. Two DO electrodes (MI-730) were used in this study, one was placed at the top of the downcomer, the other at the bottom of the fluidized-bed section in the riser. The dissolved oxygen concentration profile was recorded on a chart recorder. A model was applied to the DO profile to calculate the k_La_L value, with the assumptions of constant gas phase composition, well-mixed liquid phase, and negligible electrode response time. The first assumption is widely known and the second assumption can be justified since the DO measurements from the two different locations in the proposed reactor are quite comparable. The electrode response time was

Table 2
Particle properties and loading

Type	Density (kg m^{-3})	Average diameter (m)	Loading (kg)
Lexan	1170	3.0×10^{-3}	0.30, 0.35, 0.40
PS	1350	3.3×10^{-3}	0.30, 0.35, 0.40
Glass	2460	2.3×10^{-3}	0.30, 0.35, 0.40

obtained [22] and found to have little influence on the k_La_L value. Thus, the last assumption was satisfied.

Three different types of particles were used in the experiment. The loading and the properties of the particles are shown in Table 2.

A smaller setup was also used, of which the length of the riser and downcomer were decreased by 0.49 m. The working volume was 13.6×10^{-3} m^3. The loading of particles was adjusted accordingly. All experiments were carried out at 25 °C and atmospheric pressure.

3. Results and discussion

3.1. Gas holdup

It was observed that there was no entrainment of gas bubble into the downcomer of the proposed reactor, hence the gas holdup measured was the overall gas holdup in the riser. Fig. 2 shows the measured gas holdup varying with the gas superficial velocity in the riser, where the different series of data shown are in terms of the various solid loading and particle species. It can be seen that regardless of the effect of solid particles, the gas holdup increases with an increasing gas superficial velocity, which is in accordance with the results obtained by other researchers. For any type of particles, it is shown that the gas holdup was higher for larger solid loading than that of the smaller one. As for a given solid holdup, heavier particles yield higher gas holdups. A comparison of the standard airlift (without particles) with the reactor containing a solid bed in the riser in this study is also depicted in Fig. 2, and a net increase in gas holdup can be found in the presence of the fluidized bed. Similar observation was reported by others [20]. Decreases of the liquid circulation velocity is attributed to the fluidized bed, resulting in the increase of gas bubble residence time in the reactor, and the lowering of the liquid circulation velocity, and thus the higher the gas holdup in the riser under the same gas input. The solid lines in Fig. 2 represent the power regression of the gas holdup with the gas superficial velocity, regardless of the solid properties. The regression has the form:

$$\varepsilon = \alpha U_{Gr}^{\beta} \quad (1)$$

which was presented by Chisti [22]. It is shown that the results of gas holdup follow this equation.

When the downcomer is blocked, there will be no liquid recirculation in the reactor, the reactor can be taken as bubble column. The gas holdups under the situation of no net liquid

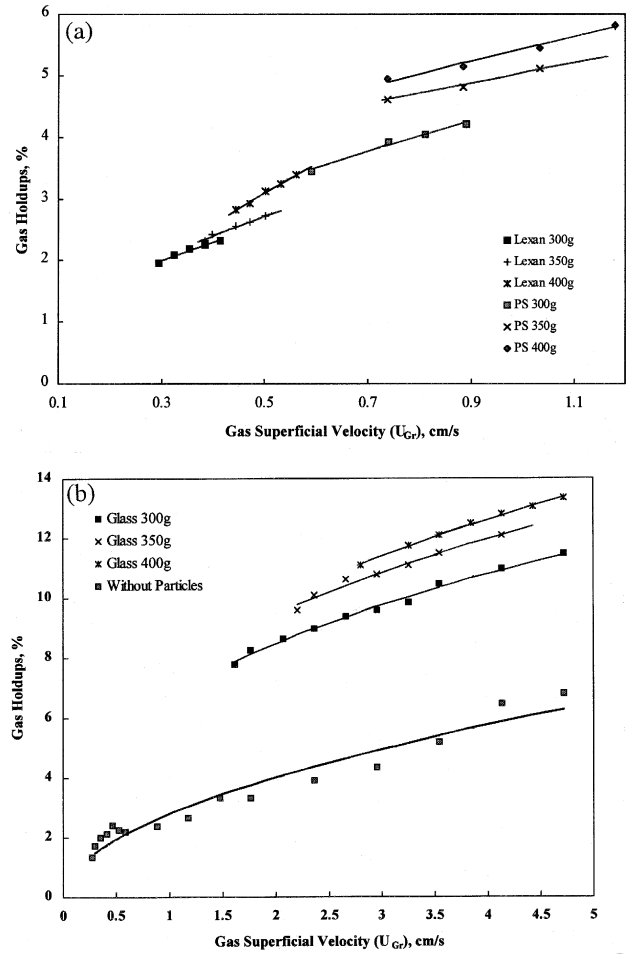

Fig. 2. (a) Variation of gas holdup with gas superficial velocity (lower range). (b) Variation of gas holdup with gas superficial velocity (higher range).

flow in the riser were also measured and plotted in Fig. 2. From the figure we can see that the gas holdups with no liquid circulation (bubble column) are actually the gas fraction at minimum fluidization (air-lift column). It can be predicted that regardless of the type and loading of particles, the gas holdup at incipient fluidization should be along the curve and those at higher gas flowrates will be located on the right-hand side of it.

The model of Zuber and Findlay [23] is widely used in the studies of gas–liquid two-phase flow to determine the gas holdups in an airlift reactor, which takes into account both the effect of non-uniform flow and gas holdup profiles as well as the effect of the slip velocity between the phases. The generally accepted form of the model is:

$$\frac{U_G}{\vec{\varepsilon}_G} = C_0(U_G + U_L) + C_1 \quad (2)$$

where U_G and U_L are the gas and liquid superficial velocity, respectively. The value of C_0 indicates the extent of radial non-uniformity in the gas holdup. C_1 is stated to be close to the rising velocity of a single bubble. The experimental data obtained in this study were used to determine the values for

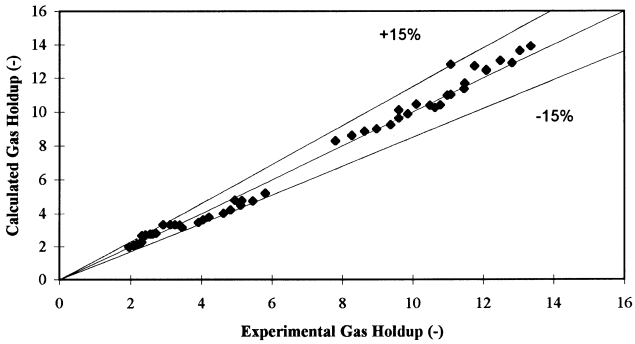

Fig. 3. Zuber and Findlay model for prediction of gas holdup.

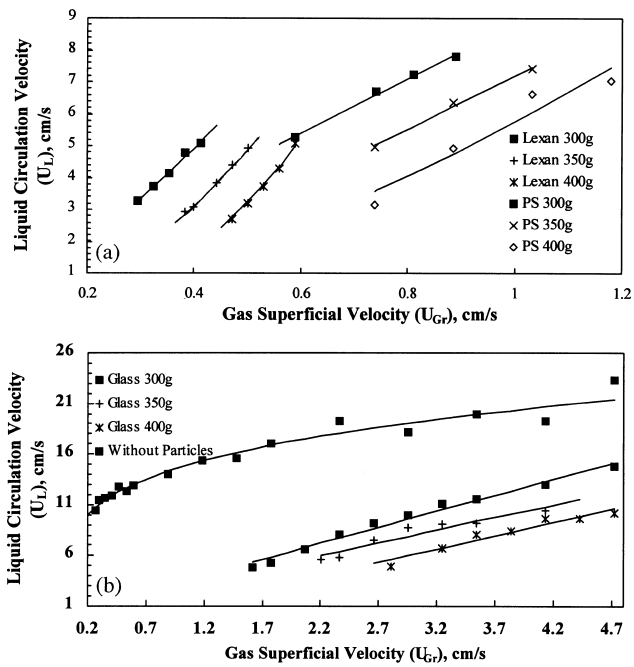

Fig. 4. (a) Variation of liquid circulation velocity with gas superficial velocity (lower range). (b) Variation of liquid circulation velocity with gas superficial velocity (higher range).

C_0 and C_1. The results were: $C_0 = 1.68$, and $C_1 = 8.82 \times 10^{-2}$ m s^{-1}. The value of C_0 is in accordance with the value of 1.6 which was reported by Zuber and Findlay [23] for an air–water mixture flowing through a circular pipe. The C_0 value obtained in this study indicates a higher concentration of bubbles in the central region of the riser, which had been observed during the experiment. The C_1 value reported in Zuber and Findlay relation was 0.25 m s^{-1} for air–water flowing through a pipe of around 0.05 m ID. In this study, however, the C_1 value was merely 0.088 m s^{-1}, which was much smaller that of the predicted one. It could be due to the location of the measuring taps, which, owing to the radial non-uniformity of the gas holdup in the riser, did not take the higher non-homogeneous region around the sparger into account, thus resulting in higher gas holdup values and obtaining lower estimates of C_1. However, the calculated gas holdup values using the Zuber and Findlay relation (Eq. (2)) were found to be compatible to the experimental data shown in Fig. 3. Good agreement can be found.

3.2. Liquid circulation velocity

In Fig. 4, the liquid circulation velocity is plotted against the gas superficial velocity, using solid loading as the parameter. The chart shows that the liquid circulation velocity increases with increasing gas superficial velocity and declines with increasing particle density and solids loading in the reactor. The same results have been reported by other researchers [24,9,14,12]. The reason for this is that an increase in solid holdup increases the solid drag and reduces the liquid circulation velocity in the reactor. For a given solid holdup, heavier particles result in higher pressure drop and hence lower liquid circulation rates.

In the solid-free two-phase flow system, the liquid circulation velocity, U_L, changes with $U_{Gr}^{0.24}$. This is in agreement with the results obtained by Choi and Lee [25], in which study, U_L varies with $U_{Gr}^{0.26}$. When the resistance to the flow of the liquid is increased by the addition of particles, the liquid circulation velocities decrease, but the exponent increases. This same trend was reported by Garnier et al. [20]

The liquid circulation velocity in the smaller setup, i.e., with lower H/D ratio (height to diameter ratio), was studied for comparison. Fig. 5 shows the results. For the two setups, although the changes in U_L for the two-phase flow systems

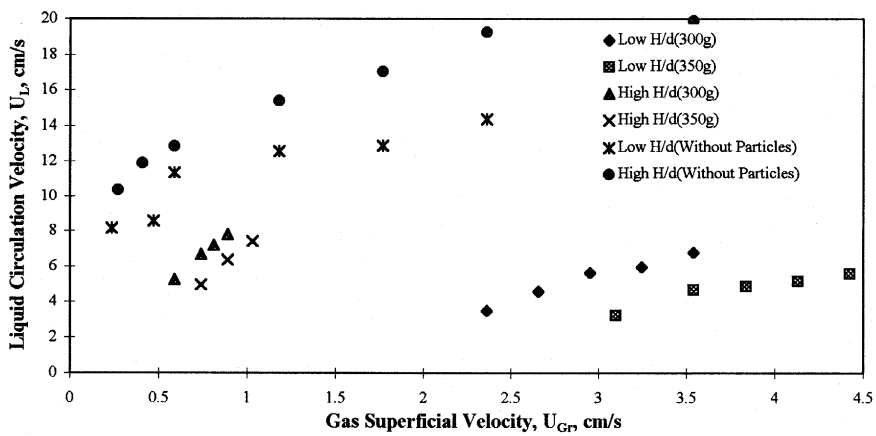

Fig. 5. Effect of H/D on U_L (PS) (High $H/D = 30.2$; low $H/D = 22.0$).

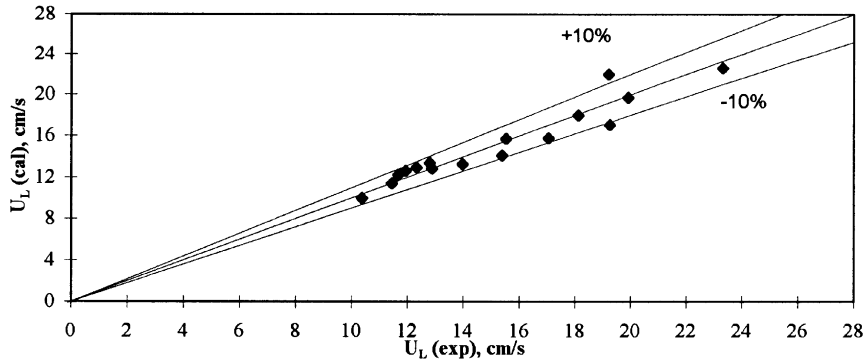

Fig. 6. Comparison of liquid circulation velocities in two-phase system predicted by Eq. (3) with the experimental data.

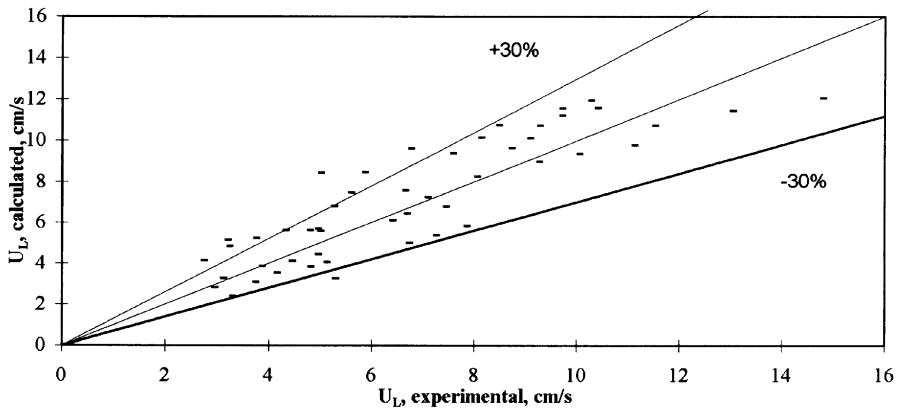

Fig. 7. Predicted U_L by Eq. (5) comparing with experimental data.

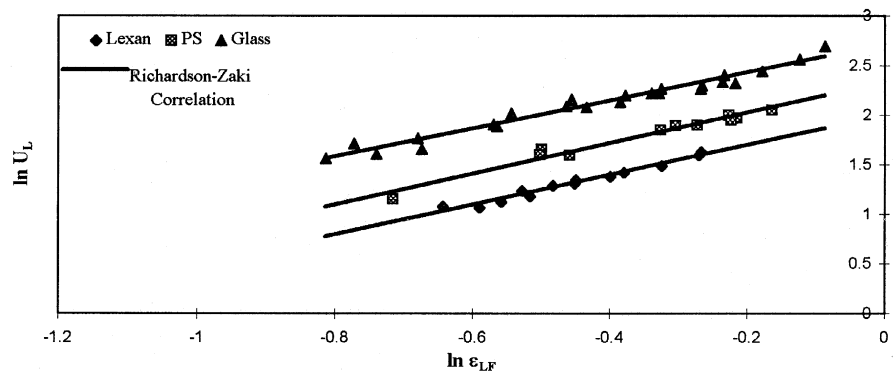

Fig. 8. Relationship of liquid circulation velocity and solid bed porosity.

Table 3
Parameters for the Richardson and Zaki Equation

Particles	n	n_{small}	U_t (cm s^{-1}), experimental	U_t (cm s^{-1}), exp. (small setup)	60% U_t (cm s^{-1}) calculated
Lexan	1.51	1.82	7.4	7.4	7.0
PS	1.55	1.64	10.3	10.1	10.3
Glass	1.42	1.48	15.0	13.5	18.8

are not too large, it is noted that the U_L value decreases drastically when the ratio of H/D is smaller at constant solid holdups in the fluidized bed. This is due to the fact the aerated height is shorter at lower H/D ratio, resulting in smaller driving force for liquid circulating.

The liquid circulation velocity in the proposed reactor in this study can be predicted using the energy balance model [26]. For gas–liquid two-phase system, the model is expressed as:

$$U_L = \left\{ \frac{2gh_D(\varepsilon_r - \varepsilon_d)}{K_B\left[\frac{1}{(1-\varepsilon_r)^2} + \left(\frac{A_r}{A_d}\right)^2 \frac{1}{(1-\varepsilon_d)^2}\right]} \right\}^{0.5} \quad (3)$$

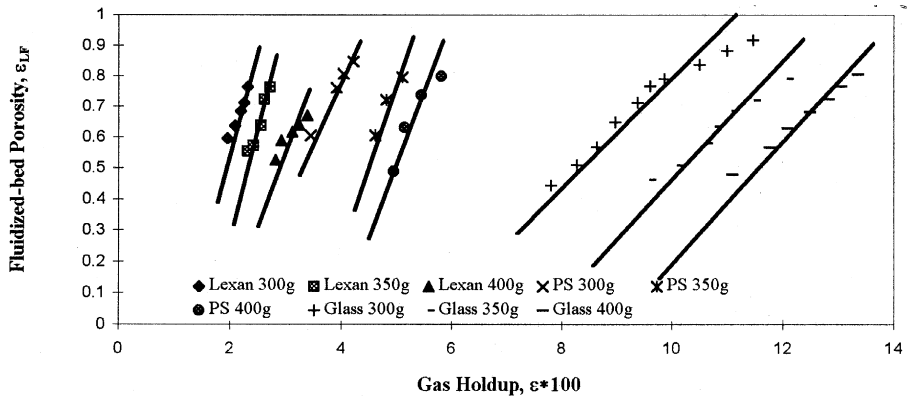

Fig. 9. Relationship between fluidized-bed porosity and gas holdup.

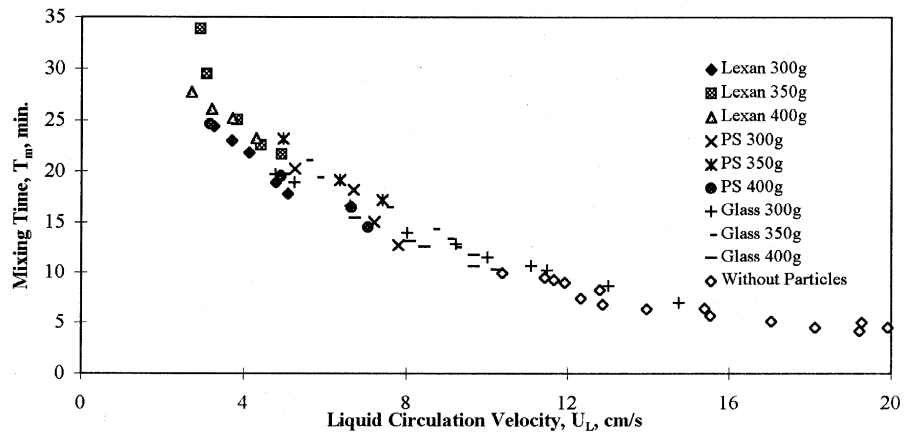

Fig. 10. Effect of liquid circulation velocity on mixing time.

The frictional loss coefficient K_B was determined by substituting all the measured values into Eq. (3). Then this measured value of U_L was compared with the calculated one in Fig. 6. In order to apply this model to predict the U_L value in three-phase systems in this study, some modification should be made to Eq. (3). As the solid particles were present, an additional energy loss existed when the liquid was passing through the fluidized bed, which is denoted as E_s here, and can be expressed as:

$$E_s = -\Delta p\, A_r U_L \tag{4}$$

The resulting equation may be written as:

$$U_L = \left\{ \frac{2gh_D(\varepsilon_r - \varepsilon_d) - 2(-\Delta p)/\rho_L}{K_B\left[\frac{1}{(1-\varepsilon_r)^2} + \left(\frac{A_r}{A_d}\right)^2 \frac{1}{(1-\varepsilon_d)^2}\right]} \right\}^{0.5} \tag{5}$$

The calculated U_L versus the experimental data is shown in Fig. 7. From Figs. 6 and 7, it can be observed that this energy balance model applies better to the gas–liquid two-phase system than to the gas–liquid–solid three-phase systems.

3.3. Fluidized bed expansion

The fluidized bed in the proposed reactor was the solid–liquid two-phase fluidization, in which bed expansion follows the Richardson–Zaki Equation [27] given by

$$(\varepsilon_{LF})^n = \frac{U_L}{U_i} \tag{6}$$

where U_i is the extrapolated liquid velocity as the bed voidage approaches 1. n is the Richardson–Zaki index. U_i is taken as the particle terminal velocity, U_t, as the particle size is negligible compared with the fluidized-bed column diameter.

The experimental results are shown in Fig. 8. It can be seen that the expansion of the fluidized bed increases with the liquid circulation velocity. The three solid lines represent the Richardson and Zaki Equation. The fluidization experiment was also carried out in the smaller setup. The parameters in the Richardson and Zaki Equation were experimentally determined and are listed in Table 3.

The experimentally obtained U_t values were found to be 60% of the theoretically calculated values [28]. This is in accordance with the results reported by Garnier et al. [20]. The parameters are shown to be comparable with those of the two reactors.

In Fig. 9 the fluidized-bed porosity is depicted as a function of the gas holdup in the riser for different solid loading and particle types. It is shown that the solid-bed porosity increases linearly with the gas holdup in the riser. And for a small change with gas holdup, the bed porosity changes sharply, especially for particles with less terminal velocities. It can be concluded that the gas holdup in the riser has a significant

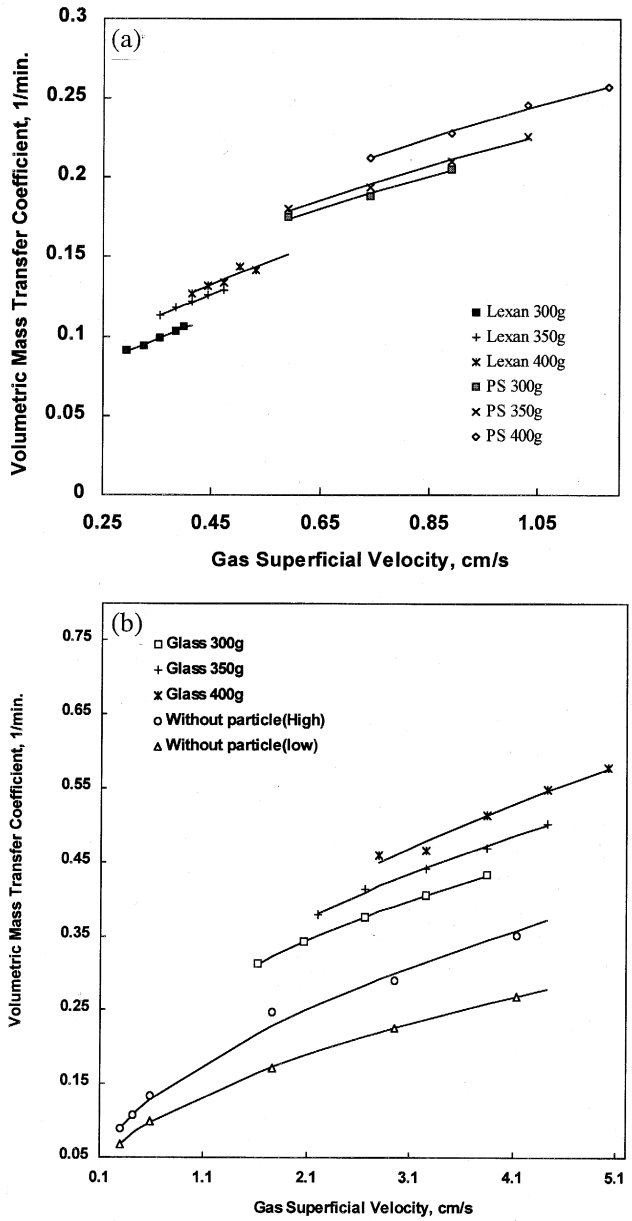

Fig. 11. (a) Volumetric mass transfer coefficient as a function of gas superficial velocity (lower range). (b) Volumetric mass transfer coefficient as a function of gas superficial velocity (higher range).

influence on the fluidized bed behaviour. At a given gas holdup the particles with smaller terminal velocity have a higher bed porosity, this is due to the smaller pressure resistance to the liquid flow.

3.4. Liquid mixing time

For given solid particles, the mixing time decreases with an increasing gas superficial velocity. In Fig. 10 the mixing time is depicted as a function of the liquid circulation velocity. It can be seen that the mixing time is in fact a variable of the liquid circulation velocity rather than a variable of the gas flowrate or the bead properties (e.g. density, shape and size). As the liquid circulation velocity increases, the mixing time decreases. Once the liquid velocity reaches a certain value, the net decline in the mixing time becomes negligible.

3.5. Mass transfer coefficient

The volumetric mass transfer coefficient k_La_L is plotted as a function of the gas superficial velocity in Fig. 11, in which different series represent different solid-bed properties. It is shown that, for a given solids, the k_La_L value increases with an increasing gas superficial velocity,which is due to the higher gas holdup in the riser caused by the larger U_{Gr}. For the same type of particles, as can be seen in the figure, the k_La_L value is higher for a larger solid loading, and as the terminal particle velocity becomes larger, the k_La_L value goes up. This is because as the particles' resistance to the liquid flow increases, the liquid circulation velocity decreases, resulting in higher gas holdup in the riser, which causes the gas–liquid mass transfer rate to increase. Fig. 12 shows that the k_La_L value varies with an increasing liquid circulation velocity in the reactor under study. The gas superficial velocity used was 0.0325 m s^{-1}. It can be seen that the mass transfer coefficient decreases as the liquid circulation velocity increases. The results shown in Fig. 12 confirm the reason discussed above.

When there were no solid particles in the proposed reactor, i.e., the standard airlift reactor mode with gas–liquid two-phase flow, the mass transfer coefficient was found to be lower than that of the reactor containing solid particles, as shown in Fig. 11. This is due to the smaller gas holdup in the two-phase reactor. The effect of H/D ratio on the gas–liquid mass transfer is also shown in the figure for the two-phase flow system. It is obvious that because the aerated height was shortened the k_La_L value became lower for the smaller H/D ratio setup. Hence, it may be deducted that the higher the aerated height is in the airlift reactor, the larger k_La_L value can be expected.

3.6. Empirical correlations

In this study, in order to establish a design basis for the proposed reactor, the main parameters, viz., the gas superficial velocity, U_{Gr}, the solid loading in the fluidized bed, φ and the ratio of the density difference between the particles and the fluid to the density of the particles were considered

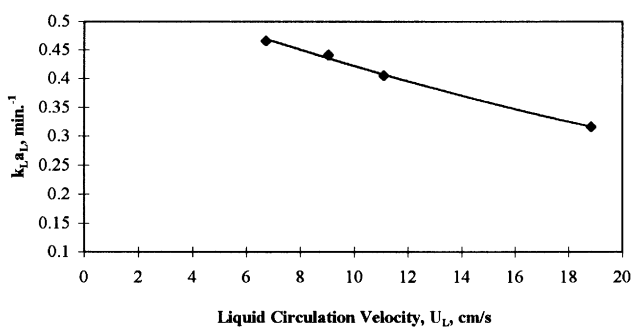

Fig. 12. Effect of U_L on k_La_L.

Table 4
Summary of empirical correlations

Correlation	Equation no.	Remarks
$\varepsilon = 101.96 U_{Gr}^{0.338} \varphi^{0.581} (1-\rho_L/\rho_p)^{0.514}$	(8)	ε in %, U_{Gr} in m s^{-1}
$U_L = 0.2041 U_{Gr}^{0.940} \varphi^{-1.393} (1-\rho_L/\rho_p)^{-0.866}$	(9)	U_L, U_{Gr} in m s^{-1}
$t_m = 424.8 U_{Gr}^{-0.871} \varphi^{1.448} (1-\rho_L/\rho_p)^{0.800}$	(10)	t_m in s, U_{Gr} in m s^{-1}
$\varepsilon = (0.493\varepsilon_{LF} + 0.438) \varphi^{1.029} (1-\rho_L/\rho_p)^{1.025}$	(11)	ε in %
$k_L a_L = 4.490 U_{Gr}^{0.384} \varphi^{0.595} (1-\rho_L/\rho_p)^{0.337}$	(12)	U_{Gr} in m s^{-1}

to describe the reactor performance. The experimental results were correlated using nonlinear regression. The correlations are summarized in Table 4. The constants in the correlation are related to the physical properties of the liquid, the geometry of the reactor as well as the gas sparger location in the reactor.

The solid loading used in the correlations was defined as the weight fraction of the particles containing within the fluidized bed, i.e.

$$\varphi = \frac{\text{Weight of Particles}}{\text{Weight of Liquid with Volume of Fluidization Column}} \quad (7)$$

The calculated results using the correlations in Table 4 were compared with the experimental data and are depicted in Figs. 13–17. Good agreement can be found.

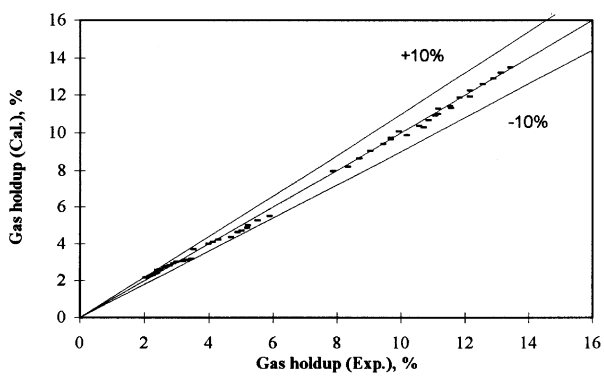

Fig. 13. Gas holdup correlation.

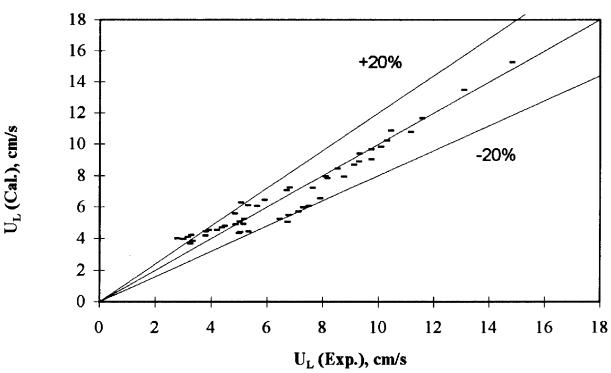

Fig. 14. Liquid circulation velocity correlation.

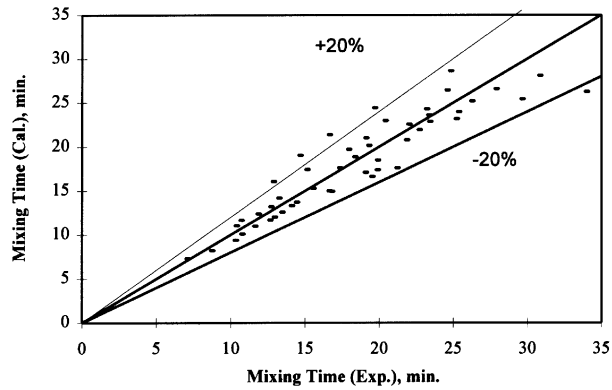

Fig. 15. Mixing time correlation.

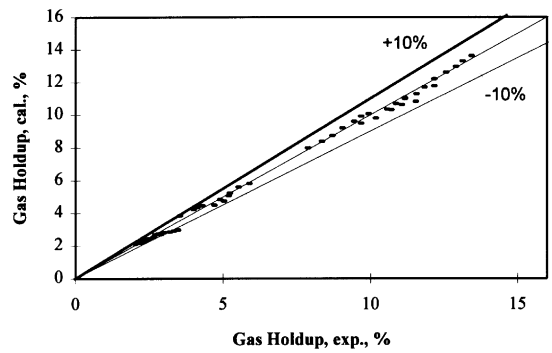

Fig. 16. Gas holdup vs. bed porosity correlation.

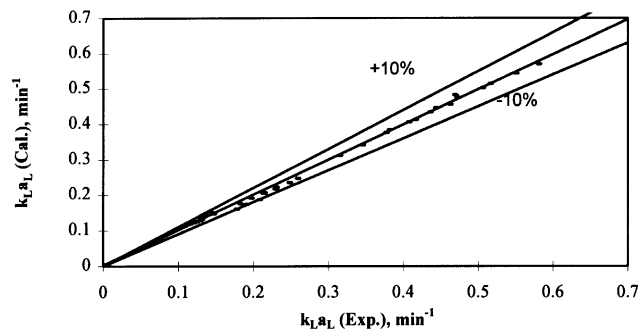

Fig. 17. Volumetric mass transfer coefficient correlation.

3.7. Possible applications

One promising application of the proposed reactor in this paper is the immobilized cell cultivation, in which the low shear rates and physical protection afforded by the immobilized matrix ensure better conditions for the growth of the fragile cells. In addition, fluidization is achieved by internal

liquid circulation, thereby avoiding the circulation of large quantities of often very costly growth media.

4. Conclusions

An external-loop airlift reactor, with fluidized bed in the riser, was studied in this work. The unique feature of the reactor is that the gas sparger is located in the middle of the riser, which permits the fluidization of heavy particles in the airlift without the intimate contact of gas and solid phases. This design can minimize the shear stress on the surface of particles. The principal application envisaged will be in immobilized cell culture. The hydrodynamic and the mass transfer performance of the proposed reactor were investigated with respect to various operating parameters such as solid loading, solid density, aerated height of the reactor, etc.

The gas holdup was found to increase with the increasing solid loading and particle densities, while the liquid circulation velocity showed the reverse trend. The mass transfer coefficient k_La_L was higher at larger gas holdup in the proposed reactor, which indicated that any attempts to improve the gas–liquid mass transfer should focus on the enhancement of the gas holdup. Some modifications to the riser-to-downcomer ratio may be made to find out the optimum configuration for the maximum mass transfer.

The proposed reactor has combined the best features of the external-loop airlift reactor and the fluidized column. It is more attractive than the conventional three-phase contactors for the following reasons:

- Low power requirements
- Low shear stresses, even when compared with the airlifts with particles circulating in the reactor. This design is more applicable to the shear-sensitive biomass cultivation.
- Heavy particles fluidizing only in the confined region, which made the reactor more flexible in the production.

The correlations describing the performance of the proposed reactor were presented in this study, which could be used for the design and scale-up of the reactor.

In view of the above, it is clear that the proposed airlift reactor with fluidized bed is expected to be a promising three-phase contactor for handling biological as well as chemical reactions, particularly in the immobilized cell culture and the enzyme processes.

5. Nomenclature

A_d	Downcomer cross-sectional area	(m^2)
A_r	Riser cross-sectional area	(m^2)
a_L	Gas–liquid interfacial area per unit liquid volume	(m^{-1})
D	Diameter of column	(m)
d_p	Diameter of particle or cell	(m)
E_s	Energy loss due to fluidized bed	(W)
g	Gravitational acceleration	($m\ s^{-2}$)
H	Height of column	(m)
h_D	Gas–liquid dispersion height	(m)
h_L	Unaerated liquid height	(m)
K_B	Frictional loss coefficient	(–)
k_L	Mass transfer coefficient	($m\ min^{-1}$)
n	A parameter	(–)
ΔP	Pressure drop	(Pa)
t_m	Mixing time	(min.)
U_G	Gas superficial velocity	($m\ s^{-1}$)
U_{Gr}	Gas superficial velocity based on riser	($m\ s^{-1}$)
U_L	Liquid superficial velocity	($m\ s^{-1}$)
U_t	Terminal particle velocity	($m\ s^{-1}$)

Greek symbols

α	A parameter	($m^{-\beta}\ s^{\beta}$)
β	Exponent	(–)
ε	Overall gas holdup	(–)
ε_d	Gas holdup in the downcomer	(–)
ε_r	Gas holdup in the riser	(–)
ε_G	Gas holdup	(–)
ε_{LF}	Void fraction of fluidized bed	(–)
ρ_L	Density of liquid	($kg\ m^{-3}$)
ρ_p	Density of solid particles	($kg\ m^{-3}$)
φ	Solid loading	($kg\ kg^{-1}$)

References

[1] P.B. Choi, Designing airlift loop fermenters, Chem. Eng. Prog. 86 (12) (1990) 32–37.
[2] Y. Chisti, M. Moo-Young, Improve the performance of airlift reactors, Chem. Eng. Prog. 89 (6) (1993) 38–45.
[3] M. Nishikawa, Biotech. Bioeng. 37 (1991) 691–692.
[4] D.G. Allen, C.W. Robinson, Biotech. Bioeng. 38 (1991) 212–216.
[5] Y. Chisti, M. Moo-Young, Prediction of liquid circulation velocity in airlift reactors with biological media, J. Chem. Tech. Biotechnol. 42 (1988) 211–219.
[6] Y. Chisti, M. Moo-Young, Hydrodynamics and oxygen transfer in pneumatic bioreactor devices, Biotech. Bioeng. 31 (1988) 487–494.
[7] R.A. Bello, C.W. Robinson, M. Moo-Young, Liquid circulation and mixing characteristics of airlift contactors, Can. J. Chem. Eng. 62 (1984) 573–577.
[8] J.C. Merchuk, I. Berzin, Distribution of energy dissipation in airlift reactors, Chem. Eng. Sci. 50 (14) (1995) 2225–2233.
[9] A.G. Livingston, S.F. Zhang, Hydrodynamic behavior of three-phase (gas–liquid–solid) airlift reactors, Chem. Eng. Sci. 48 (9) (1993) 1641–1654.
[10] H.H. Mao, Y. Chisti, M. Moo-Young, Multiphase hydrodynamics and solid–liquid mass transport in an external-loop airlift reactor—a comparative study, Chem. Eng. Commun. 113 (1992) 1–13.
[11] Wen-Jang Lu, Shyh-jye Hwang, Chun-Min Chang, Liquid mixing in two- and three-phase airlift reactors, Chem. Eng. Sci. 49 (9) (1994) 1465–1468.
[12] W.J. Lu, S.J. Hwang, C.M. Chang, Liquid mixing in internal loop airlift reactors, Ind. Eng. Chem. Res. 33 (1994) 2180–2186.
[13] B. Obradovic, A. Dudukovic, G. Vunjak-Novakovic, Local and overall mixing characteristics of the gas–liquid–solid airlift reactor, Ind. Eng. Chem. Res. 33 (1994) 698–702.

[14] R.S. Douek, A.G. Livingston, A.C. Johansson, G.F. Hewitt, Hydrodynamics of an external-loop three-phase airlift (TPAL) reactor, Chem. Eng. Sci. 49 (22) (1994) 3719–3737.
[15] E. Saunder, S. Ledakdwicz, W.D. Decker, Can. J. Chem. Eng. 64 (1986) 133–140.
[16] D.W. Murhammer, C.F. Goochee, Sparged animal cell bioreactors: Mechanism of cell damage and pluronic F-68 protection, Biotechnol. Progr. 6 (1990) 391–397.
[17] J.J. Heijnen, A. Mulder, W. Enger, F. Hoeks, Chem. Eng. J. 41 (1989) B37–B50.
[18] K. Schügerl, Nonmechanically agitated bioreactor systems, in: M. Moo-Young, C.L. Cooney, A.E. Humphrey (eds.), Comprehensive Biotechnology, vol. 2, Pergamon, Oxford, 1985, pp. 99–118.
[19] L.N. Nikolov, D.G. Karamanev, D.G. Elenkov, Bulg. Patent 53798, 1982.
[20] A. Garnier, C. Chavarie, G. Andre, D., The inverse fluidization airlift bioreactor, Part I: hydrodynamic studies, Chem. Eng. Comm. 98 (1990) 31–45.
[21] S.S. Lele, J.B. Joshi, Modeling of air-lift fluidized bed: optimization of mass transfer with respect to design and operational parameters, Chem. Eng. J. 49 (1992) 89–105.
[22] M.Y. Chisti, Airlift Bioreactors, Elsevier Science Ltd, London and New York, 1989.
[23] N. Zuber, J.A. Findlay, Average volumetric concentration in two-phase flow systems, J. Heat Tran., 87 (Nov. 1965) 453–468.
[24] Y. Bando, M. Nishimura, H. Sota, M. Hattori, N. Sakai, M. Kuraishi, J. Chem. Eng. Jpn. 23 (1990) 587–592.
[25] K.H. Choi, W.K. Lee, Circulation liquid velocity, gas holdup and volumetric oxygen transfer coefficient in external-loop airlift reactors, J. Chem. Tech. Biotechnol. 56 (1993) 51–58.
[26] M.Y. Chisti, B. Halard, M. Moo-Young, Liquid circulation in airlift fermentors, Chem. Eng. Sci. 43 (1988) 451–457.
[27] J.F. Richardson, W.N. Zaki, Sedimentation and fluidisation: part I, Trans. Inst. Chem. Eng. 32 (1954) 35–53.
[28] D. Kunii, O. Levenspiel, Fluidization Engineering, Wiley, New York, 1969, pp. 74–78.